Kneelike Structure in the Spectrum of the Heavy Component of Cosmic Rays Observed with KASCADE-Grande

W. D. Apel,[1] J. C. Arteaga-Velázquez,[2] K. Bekk,[1] M. Bertaina,[3] J. Blümer,[1,4] H. Bozdog,[1] I. M. Brancus,[5] P. Buchholz,[6] E. Cantoni,[3,7] A. Chiavassa,[3] F. Cossavella,[4,*] K. Daumiller,[1] V. de Souza,[8] F. Di Pierro,[3] P. Doll,[1] R. Engel,[1] J. Engler,[1] M. Finger,[4] D. Fuhrmann,[9] P. L. Ghia,[7] H. J. Gils,[1] R. Glasstetter,[9] C. Grupen,[6] A. Haungs,[1,‖] D. Heck,[1] J. R. Hörandel,[10] D. Huber,[4] T. Huege,[1] P. G. Isar,[1,†] K.-H. Kampert,[9] D. Kang,[4] H. O. Klages,[1] K. Link,[4] P. Łuczak,[11] M. Ludwig,[4] H. J. Mathes,[1] H. J. Mayer,[1] M. Melissas,[4] J. Milke,[1] B. Mitrica,[5] C. Morello,[7] G. Navarra,[3,‡] J. Oehlschläger,[1] S. Ostapchenko,[1,§] S. Over,[6] N. Palmieri,[4] M. Petcu,[5] T. Pierog,[1] H. Rebel,[1] M. Roth,[1] H. Schieler,[1] F. G. Schröder,[1] O. Sima,[12] G. Toma,[5] G. C. Trinchero,[7] H. Ulrich,[1] A. Weindl,[1] J. Wochele,[1] M. Wommer,[1] and J. Zabierowski[11]

(KASCADE-Grande Collaboration)

[1]*Institut für Kernphysik, Karlsruher Institut für Technologie, Karlsruhe, Germany*
[2]*Universidad Michoacana, Instituto de Física y Matemáticas, Morelia, Mexico*
[3]*Dipartimento di Fisica, Università Torino, Torino, Italy*
[4]*Institut für Experimentelle Kernphysik, Karlsruher Institut für Technologie, Karlsruhe, Germany*
[5]*National Institute of Physics and Nuclear Engineering, Bucharest, Romania*
[6]*Fachbereich Physik, Universität Siegen, Germany*
[7]*Istituto di Fisica dello Spazio Interplanetario, INAF, Torino, Italy*
[8]*Instituto de Física de São Carlos, Universidade São Paulo, São Carlos, Brasil*
[9]*Fachbereich Physik, Universität Wuppertal, Wuppertal, Germany*
[10]*Department of Astrophysics, Radboud University Nijmegen, Nijmegen, The Netherlands*
[11]*National Centre for Nuclear Research, Lodz, Poland*
[12]*Department of Physics, University of Bucharest, Bucharest, Romania*

(Received 21 July 2011; revised manuscript received 25 August 2011; published 20 October 2011)

We report the observation of a steepening in the cosmic ray energy spectrum of heavy primary particles at about 8×10^{16} eV. This structure is also seen in the all-particle energy spectrum, but is less significant. Whereas the ''knee'' of the cosmic ray spectrum at 3–5 $\times$ 10^{15} eV was assigned to light primary masses by the KASCADE experiment, the new structure found by the KASCADE-Grande experiment is caused by heavy primaries. The result is obtained by independent measurements of the charged particle and muon components of the secondary particles of extensive air showers in the primary energy range of 10^{16} to 10^{18} eV. The data are analyzed on a single-event basis taking into account also the correlation of the two observables.

DOI: 10.1103/PhysRevLett.107.171104 PACS numbers: 98.70.Sa, 95.85.Ry, 96.50.sb, 96.50.sd

The determination of the primary energy and composition in the energy range from 10^{15} up to above 10^{20} eV has been the subject of earthbound experiments for more than five decades. It has been shown that the high-energy all-particle spectrum has a power-law–like behavior ($\propto E^{\gamma}$, $\gamma \approx -2.7$), with features known as the ''knee'' at 3–5 $\times$ 10^{15} eV and the ''ankle'' at 4–10 $\times$ 10^{18} eV, respectively. Whereas at the knee the spectrum steepens ($\Delta\gamma = -0.3$–0.4), the ankle is characterized by a flattening of the spectrum ($\Delta\gamma = +0.3$–0.4). The KASCADE experiment has shown that the knee is due to a distinct decrease in the flux of primaries with light mass ($Z < 6$) [1,2]. Many astrophysical models commenting on the origin of the knee assume a dependence of such break offs (knees) on the charge of the primary nuclei [3,4]. Assuming that the knee is related to a break in the spectrum of primary hydrogen nuclei, a kneelike structure in the spectrum of the heavy component ($Z > 13$ up to iron nuclei) is expected in the energy range from about 4×10^{16} to about 1.2×10^{17} eV. So far, such a structure has not been observed experimentally. We present measurements of extensive air showers (EAS) in the primary energy range of 10^{16} to 10^{18} eV performed with KASCADE-Grande (KArlsruhe Shower Core and Array DEtector with Grande extension) and investigate the mass composition of the cosmic rays.

KASCADE-Grande, located at 49.1°N, 8.4°E, 110 m above sea level, consists of the Grande array with 37 stations of 10 m^2 scintillation detectors each, spread over an area of 700×700 m^2, the original KASCADE array covering 200×200 m^2 with unshielded and shielded detectors, a muon tracking device, and a large calorimeter [5,6]. This multidetector system allows us to investigate in detail the EAS generated by high-energy primary cosmic rays in the atmosphere. For the present analysis, the

estimation of energy and mass of the primary particles is based on the combined measurement of the charged particle component by the detector array of Grande and the muon component by the KASCADE muon array (Fig. 1). Basic shower observables like the core position, zenith angle, and total number of charged particles (shower size N_{ch}) are derived from the measurements of the Grande stations. While the Grande detectors are sensitive to charged particles, the muonic component is measured independently by the shielded detectors of the KASCADE array. 192 scintillation detectors of 3.24 m^2 sensitive areas each are placed below an iron and lead absorber to select muons above 230 MeV kinetic energy. A core position resolution of 5 m, a direction resolution of 0.7°, and a resolution of the shower size of about 15% are achieved. The total number of muons (N_μ) with a resolution of about 25% is calculated by combining the core position determined by the Grande array and the muon densities measured at the KASCADE array, where N_μ undergoes a correction for a bias in reconstruction due to the asymmetric position of the detectors [5].

The present analysis is based on 1173 days of data taking. The cuts on the sensitive area (EAS core reconstructed within the array) and zenith angle ($< 40°$), chosen to assure best and constant reconstruction accuracies, result in an exposure of 2×10^{13} $m^2 \times s\,sr$. Figure 2 displays the correlation of the two observables N_{ch} and N_μ. This distribution is the basis of the following analysis, since it contains all the experimental information required for reconstructing the energy and mass of the cosmic rays: the higher the energy of the primary cosmic ray the larger the total particle number. The fraction of muons of all charged particles at observation level is characteristic for the primary mass: showers induced by heavy primaries start earlier in the atmosphere and the higher nucleon number leads to a relatively larger muon content at observation level. KASCADE-Grande measures the particle number at an atmospheric depth well beyond the shower maximum, where the electromagnetic component already becomes reduced. Thus, electron-rich EAS are generated preferentially by light primary nuclei and electron-poor EAS by heavy nuclei, respectively.

However, a straightforward analysis is hampered by the shower-to-shower fluctuations, i.e., by the dispersion of the muon and electromagnetic particle numbers for a fixed primary mass and energy. In addition, cosmic rays impinging on the atmosphere under different zenith angles show a varying, complicated behavior due to the nonuniform mass and density distribution of the air. Therefore, the absolute energy and mass scale have to be inferred from comparisons of the measurements with Monte Carlo simulations. This creates additional uncertainties, since the physics of

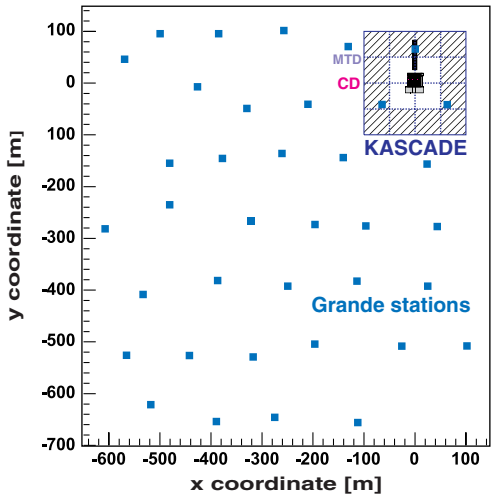

FIG. 1 (color online). Layout of the KASCADE-Grande experiment: shown are the Grande array as well as the KASCADE array with its central detector (CD) and muon tracking detector (MTD). The shaded area marks the outer 12 clusters (16 detector stations each) of the KASCADE array consisting of shielded (muon array) and unshielded detectors. The inner 4 clusters consist of unshielded detectors only.

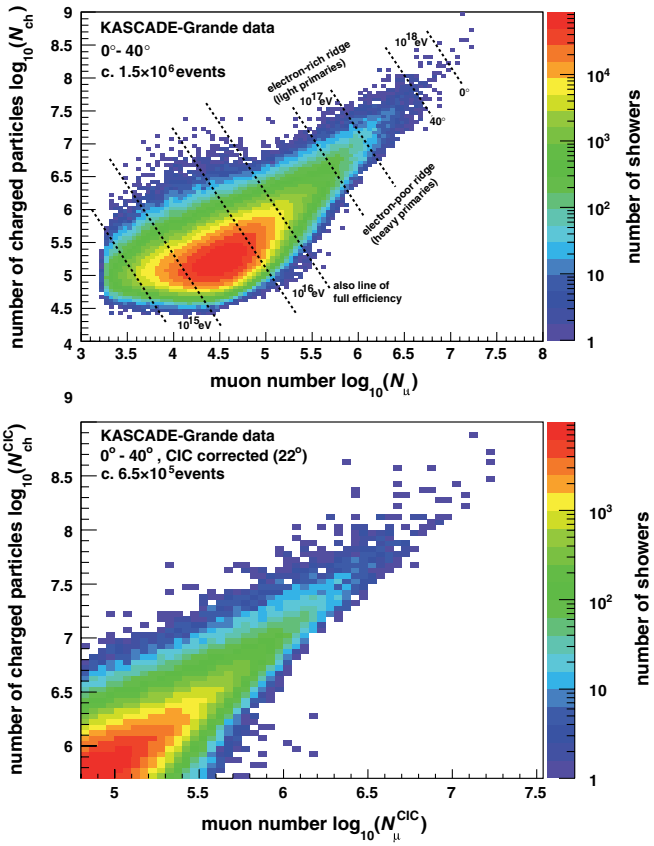

FIG. 2 (color online). Two-dimensional distribution of the shower sizes: charged particle number and total muon number. All quality cuts are applied. In addition, a roughly estimated energy scale is indicated in the upper panel. The lower panel shows a zoom to higher energies of the same observables, which is now corrected for attenuation.

the relevant particle interactions is not completely tested by man-made accelerator experiments. The uncertainties imposed by the hadronic interaction models are more relevant for composition analyses than for energy measurements. Hence, our strategy is to separate the measured EAS in electron-poor and electron-rich events as representatives of the heavy and light primary mass groups, similar to the analysis presented in Ref. [1]. The shape and structures of the resulting energy spectra of these individual mass groups are much less affected by the differences of the various hadronic interaction models than the relative abundance.

As a consequence of the considerations above, the energy and mass assignment of individual events is achieved by using both observables N_{ch} and N_{μ}, as well as their correlation. The following equation is motivated by discussions of hadronic air showers in Ref. [7], with the basic idea that the total number of secondary particles at observation level is related to the primary energy while the energy sharing between the electromagnetic and the hadronic (i.e. muonic) shower components is related to the primary mass. Therefore, the primary energy $\log_{10}(E)$ is assumed to be proportional to the shower size $\log_{10}(N_{\mathrm{ch}})$ with a correction factor that accounts for the mass dependence by making use of the measured ratios of shower sizes $\log_{10}(N_{\mathrm{ch}}/N_{\mu})$:

$$\log_{10}(E/GeV) = [a_{\mathrm{H}} + (a_{\mathrm{Fe}} - a_{\mathrm{H}})k]\log_{10}(N_{\mathrm{ch}}) + b_{\mathrm{H}} + (b_{\mathrm{Fe}} - b_{\mathrm{H}})k, \quad (1)$$

$$k = \frac{\log_{10}(N_{\mathrm{ch}}/N_{\mu}) - \log_{10}(N_{\mathrm{ch}}/N_{\mu})_{\mathrm{H}}}{\log_{10}(N_{\mathrm{ch}}/N_{\mu})_{\mathrm{Fe}} - \log_{10}(N_{\mathrm{ch}}/N_{\mu})_{\mathrm{H}}}, \quad (2)$$

with $\log_{10}(N_{\mathrm{ch}}/N_{\mu})_{\mathrm{H,Fe}} = c_{\mathrm{H,Fe}} \times \log_{10}(N_{\mathrm{ch}}) + d_{\mathrm{H,Fe}}$. The parameter k takes into account both the average differences in the N_{ch}/N_{μ} ratio among different primaries with the same N_{ch} as well as the shower-to-shower fluctuations for events of the same primary mass. The exact form of the equation is optimized for the experimental situation of KASCADE-Grande and the free parameters [8] are determined by Monte Carlo simulations [9]. They are defined independently for 5 different zenith angle intervals of equal exposure (the upper limits of θ are 16.7°, 24.0°, 29.9°, 35.1°, and 40.0°) to take into account the shower attenuation. Data are combined only at the very last stage to reconstruct the final energy spectrum. The N_{ch}-N_{μ} correlation of individual events is incorporated in calculating k, which serves now as mass sensitive observable. Figure 3 shows the evolution of k as a function of the reconstructed energy for the first two zenith angle bins, where a similar behavior is observed for all angular ranges. The error bars include statistical as well as reconstruction uncertainties of the k parameter. The width of the k distributions decreases slightly for increasing energy and amounts, at 100 PeV, to about ± 0.2, ± 0.15, ± 0.4 for H, Fe, and data, respectively.

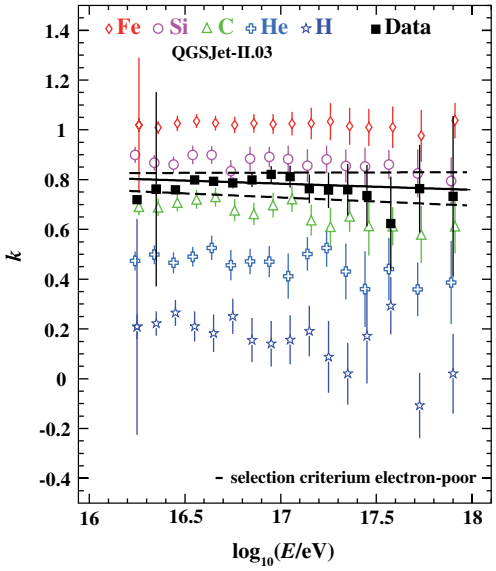

FIG. 3 (color online). Evolution of the k parameter as a function of the reconstructed energy for experimental data compared with simulations of primary masses for the angular range 0°–24°. The error bars assign statistical as well as reconstruction uncertainties of k. The line displays the chosen energy dependent k values for separating the mass groups, where the dashed lines assign the uncertainty of the selection.

The k parameter is used to separate the events into different samples. The line in Fig. 3 separates the electron-poor (heavy) group, and is defined by fitting the $k_{\mathrm{ep}}(E) = [k_{\mathrm{Si}}(E) + k_{\mathrm{C}}(E)]/2$ distribution. The dashed lines represent the uncertainties in defining this energy dependent selection cut. The resulting spectra are shown in Fig. 4, where the band indicates changes of the spectra when the cut is varied within the dashed lines shown in Fig. 3. The energy resolution for an individual event is better than 25% over the entire energy range and the all-particle spectrum is reconstructed within a total systematic uncertainty in flux of 10%–15% [8,10].

The reconstructed spectrum of the electron-poor events shows a distinct kneelike feature at about 8×10^{16} eV. Applying a fit of two power laws to the spectrum interconnected by a smooth knee [11] results in a statistical significance of 3.5σ that the entire spectrum cannot be fitted with a single power-law. The change of the spectral slope is $\Delta\gamma = -0.48$ from $\gamma = -2.76 \pm 0.02$ to $\gamma = -3.24 \pm 0.05$ with the break position at $\log_{10}(E/eV) = 16.92 \pm 0.04$. Applying the same function to the all-particle spectrum results in a statistical significance of only 2.1σ that a fit of two power laws is needed to describe the spectrum. Here the change of the spectral slope is from $\gamma = -2.95 \pm 0.05$ to $\gamma = -3.24 \pm 0.08$, but with the break position again at $\log_{10}(E/eV) = 16.92 \pm 0.10$. Hence, the selection of heavy primaries enhances the kneelike feature that is already present in the all-particle spectrum. The spectrum of the electron-rich events (light

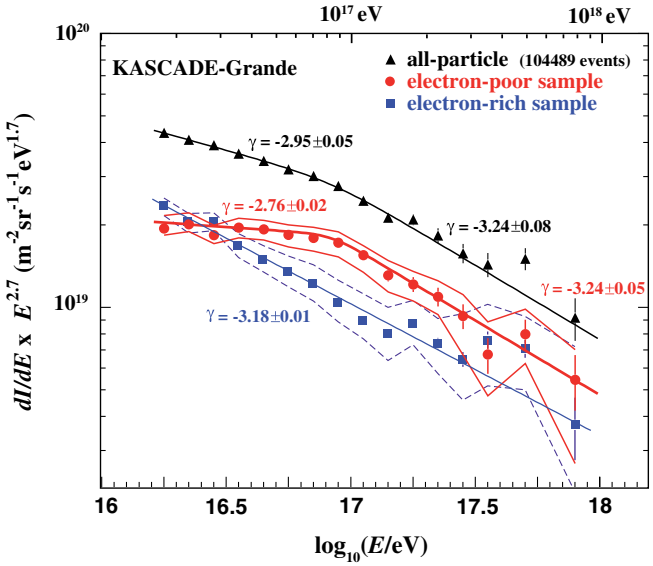

FIG. 4 (color online). Reconstructed energy spectrum of the electron-poor and electron-rich components together with the all-particle spectrum for the angular range 0°–40°. The error bars show the statistical uncertainties; the bands assign systematic uncertainties due to the selection of the subsamples. Fits on the spectra and resulting slopes are also indicated.

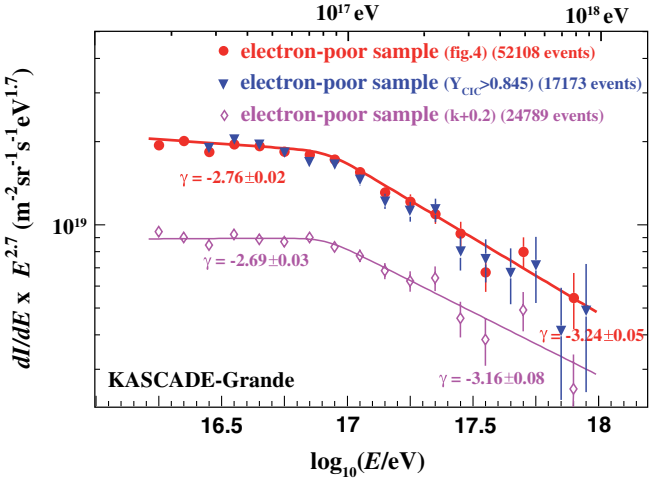

FIG. 5 (color online). Energy spectra of electron-poor (heavy) event samples obtained by different selection and reconstruction criteria. The original spectrum from Fig. 4 is compared with the spectrum from a more selective cut in the k parameter and with the spectrum obtained by using the Y_{CIC} parameter for selecting the electron-poor events (see text).

and medium mass primaries) is compatible with a single power law with slope index $\gamma = -3.18 \pm 0.01$. However, a recovery to a harder spectrum at energies well above 10^{17} eV cannot be excluded by the present data. This finding is of particular interest and needs more detailed investigations with improved statistics in future.

The main result, i.e., the kneelike structure in the spectrum of electron-poor events, is validated in the following by various cross checks (Fig. 5). Variations of the slopes of the selection cut, as well as parallel shifts of the cut lines have shown that the spectral form, i.e., the kneelike structure of the electron-poor event sample, is retained. By shifting k to larger values the fraction of heavy primaries in the sample is enriched. Interestingly, we found that the slope index of the spectrum is not significantly changing beyond the break, but gets systematically harder at lower energies. The position of the break remains constant, indicating that the heaviest primaries in the sample dominate the spectral form. An example of a spectrum obtained by such a variation of the selection cut is shown in Fig. 5.

A systematic uncertainty possibly affecting the interpretation of the data is related to the attenuation of the particle numbers in the atmosphere. So far, the attenuation given by the EAS simulations is taken into account. For validation, an independent analysis is performed where the correction for attenuation, i.e., for the zenith angular dependence, is based on the measured events, and not on simulations. The correction parameters are obtained by applying the constant intensity cut method (CIC) [12] to the two observables independently. This procedure allows the data collected from different zenith angles to be combined in a model independent way. The shower size ratio $Y_{\mathrm{CIC}} = \log_{10} N'_{\mu} / \log_{10} N'_{\mathrm{ch}}$ is calculated, where N'_{μ} and N'_{ch} are the shower sizes corrected for attenuation effects in the atmosphere in such a way that they correspond to the shower sizes at a certain reference zenith angle. In order to check, in addition to the attenuation correction, also reconstruction and selection uncertainties, we applied more stringent cuts for this analysis, which increase the energy threshold and decrease the statistics of the event sample compared to the standard analysis. Now, Y_{CIC} is used to separate the events into electron-rich and electron-poor subsamples. In contrast to the k parameter, the Y_{CIC} parameter is almost energy independent, where the energy of the individual events is again determined using Eq. (1). For direct comparison with the results obtained before, $Y_{\mathrm{CIC}} > 0.845$ is chosen for selecting the electron-poor event sample. The reconstructed spectrum (see Fig. 5) obviously confirms the earlier finding of the kneelike structure, which is due to a decrease in the flux of the heavy component.

Another source of systematic uncertainty is related to the hadronic interaction model. In the frame of QGSJet-II, the measured distributions in k and Y_{CIC} are in agreement with a dominant electron-poor composition for the entire energy range. Whereas the Y_{CIC} and k values themselves behave differently for other hadronic interaction models, the measured and simulated Y_{CIC} and k dependences on energy, and hence the shapes and structures of the resulting spectra are similar [13]. Details will be discussed in a forthcoming paper, but it is not expected that the basic result of the present analysis changes.

Summarizing, by dividing KASCADE-Grande measured air-shower events in electron-rich and electron-poor subsamples, there is first evidence that at about 8×10^{16} eV the spectrum of the heavy component of primary cosmic rays shows a kneelike break. The spectral steepening occurs at an energy where the charge dependent knee of primary iron is expected, when the knee at about $3–5 \times 10^{15}$ eV is assumed to be caused by a decrease in the flux of primary protons.

The authors would like to thank the members of the engineering and technical staff of the KASCADE-Grande Collaboration who contributed to the success of the experiment. KASCADE-Grande is supported by the BMBF of Germany, the MIUR and INAF of Italy, the Polish Ministry of Science and Higher Education (grant for the years 2009–2011), and the Romanian Authority for Scientific Research UEFISCDI, (Grants No. PNII-IDEI 1442/2008 and No. PN 09 37 01 05). J. C. A., A. H., and M. F. acknowledge partial support from the DAAD-Proalmex program (2009–2010), and J. C. A. from CONACYT and the Consejo de la Investigación Científica of the Universidad Michoacana.

*Present address: Max-Planck-Institut für Physik, München, Germany.
†Present address: Institute of Space Sciences, Bucharest, Romania.
‡Deceased.
§Present address: University of Trondheim, Norway.
‖haungs@kit.edu

[1] T. Antoni *et al.* (KASCADE Collaboration), Astropart. Phys. **16**, 373 (2002).
[2] T. Antoni *et al.* (KASCADE Collaboration), Astropart. Phys. **24**, 1 (2005).
[3] B. Peters, Nuovo Cimento **22**, 800 (1961).
[4] J. R. Hoerandel, Astropart. Phys. **21**, 241 (2004).
[5] W.-D. Apel *et al.* (KASCADE-Grande Collaboration), Nucl. Instrum. Methods Phys. Res., Sect. A **620**, 202 (2010).
[6] T. Antoni *et al.* (KASCADE Collaboration), Nucl. Instrum. Methods Phys. Res., Sect. A **513**, 490 (2003).
[7] J. Matthews, Astropart. Phys. **22**, 387 (2005).
[8] M. Bertaina *et al.* (KASCADE-Grande Collaboration), Astrophys. Space Sci. **7**, 229 (2011).
[9] Simulations include the full air-shower development in the atmosphere and the response of the detector [14]. The EAS were generated using CORSIKA [15] and the models FLUKA [16] and QGSJet-II.03 [17] in the energy range from 10^{15} to 3×10^{18} eV for five different representative mass groups: H, He, C, Si, and Fe with about 353.000 events per primary.
[10] The resulting spectra for the present analysis are not corrected for reconstruction uncertainties. But, more detailed investigations [8] have shown that the effects are smaller than the estimated uncertainty on the flux of 10%–15%. In addition, the absolute energy scale depends on the used hadronic interaction model, e.g., for EPOS v1.99 [18] a 10%–15% lower flux in the all-particle spectrum is obtained.
[11] T. Antoni *et al.* (KASCADE Collaboration), Astropart. Phys. **16**, 245 (2002).
[12] J. Hersil *et al.*, Phys. Rev. Lett. **6**, 22 (1961); D. M. Edge *et al.*, J. Phys. A **6**, 1612 (1973).
[13] First analyses based on simulations with the hadronic interaction model EPOS v1.99 [18] have confirmed the findings of the kneelike feature in the spectrum of the heavy component for both analysis approaches, though the relative abundance of the subsamples change considerably.
[14] CERN, GEANT 3.21, Detector Description and Simulation Tool, CERN Program Library Long Writeup W5015, 1993.
[15] D. Heck *et al.*, Forschungszentrum Karlsruhe Report No. FZKA 6019, 1998.
[16] A. Fassò *et al.*, Report No. CERN-2005-10, INFN/TC-05/11, SLAC-R-773, 2005.
[17] S. S. Ostapchenko, Nucl. Phys. B, Proc. Suppl. **151**, 143 (2006); S. Ostapchenko, Phys. Rev. D **74**, 014026 (2006).
[18] K. Werner, F. M. Liu, and T. Pierog, Phys. Rev. C **74**, 044902 (2006).